Earth-mass dark-matter haloes as the first structures in the early Universe

J. Diemand[1*], B. Moore[1] & J. Stadel[1],

[1] Institute for Theoretical Physics, University of Zurich, Winterthurerstrasse 190, CH-8057 Zürich, Switzerland

Before a redshift z=100, about 20 million years after the big bang, the universe was nearly smooth and homogenous.[1] After this epoch tiny fluctuations imprinted in the matter distribution during the initial expansion began to collapse via gravitational instability. The properties of these fluctuations depend on the unknown nature of dark matter,[2–4] which is one of the biggest challenges in present day science.[5–7] Here we present supercomputer simulations of the concordance cosmological model assuming neutralino dark matter and find the first objects to form are numerous earth mass dark matter halos about as large as the solar system. They are stable against gravitational disruption, even within the central regions of the Milky Way, and we expect over 10^{15} to survive within the Galactic halo with one passing through the solar system every few thousand years. The nearest structures will be amongst the brightest sources for gamma-rays from particle-particle annihilation.

The cosmological parameters of our universe and initial conditions for structure formation have recently been measured via a combination of observations including the cosmic microwave background (CMB)[8] , distant supernovae[9,10] and the large scale distribution of galaxies.[11] Cosmologists now face the outstanding problem of understanding the origin of structure in the universe from its strange mix of particles and vacuum energy.[12,13]

Most of the mass of the universe must be a non-baryonic particle[1,14] that remains undetected in laboratory experiments. The leading candidate for this "dark matter" is the neutralino, the lightest supersymmetric particle which is predicted to solve several key

*Present adress: Department of Astronomy Astrophysics, University of California, 1156 High Street, Santa Cruz CA 95064, USA

problems in the standard model for particle physics.[5] This cold dark matter (CDM) candidate is not completely collisionless. It can collide with baryons thus revealing its presence in laboratory detectors, although the cross-section for this interaction is extremely small. In a cubic meter detector containing $\sim 10^{30}$ baryon particles only a few collisions per day are expected from the $\sim 10^{13}$ dark matter particles that flow through the experiment as the earth moves through the galaxy. The neutralino is its own anti-particle and it can self-annihilate creating a shower of new particles including gamma-rays.[5] The annihilation rate increases as the density squared therefore the central regions of the Galaxy and its satellites will give the strongest signal.[15–18] However the expected rate is very low - the flux of photons on earth is the same as we would receive from a single candle placed on Pluto. Numerous experiments utilising these effects are underway which may detect the neutralino within the next decade.[7] Furthermore, in the next few years the LHC at CERN will confirm or rule out the concepts of supersymmetry (SUSY).[6]

We followed the growth and subsequent gravitational collapse and virialisation of the first structures in the cold dark matter universe with supercomputer calculations. The challenge is to accurately follow the evolution of the universe on scales that are many orders of magnitude smaller than previously studied, whilst also capturing the gravitational dynamics from large scales. We use a multiscale technique[19] in order to achieve the desired resolution within a small average density patch of the universe which is nested within a hierarchy of larger and lower resolution grids of particles.

The fluctuations are imposed on the particles using accurate calculations of the linear theory power spectrum for a SUSY model with a particle mass $m_\nu = 100$ GeV. This includes collisional damping, free streaming and the transfer of fluctuations through the matter-radiation era of the universe.[2–4] The resulting power spectrum is close to a power law $P(k) \propto k^n$ with $n = -3$ with an exponential cut-off at 0.6 comoving parsecs which corresponds to a mass scale of $10^{-6} M_\odot$. The cutoff scale depends on the neutralino mass and decoupling energy. From accelerator searches we know that $m_\nu > 37$ GeV and the cosmic matter density sets an upper limit at 500 GeV. The damping scale for the allowed neutralino models differ from the model we used by less than a factor of three in mass[2–4] and therefore structure formation is very similar in all SUSY-CDM scenarios. A less popular CDM candidate is the axion, it has a much smaller damping scale of

$10^{-13} M_{\odot}$. For comparison we simulated the high resolution region with an axion CDM fluctuation spectrum on the resolved scales. Both models produce equal halo abundances above $5 \times 10^{-6} M_{\odot}$, but the axion model also forms bound structures down to the smallest resolved scales, see Figure 3. In this letter we concentrate on the properties of the first structures to form in the SUSY-CDM model.

We evolve the initial particle distribution using a parallel multi-stepping treecode, starting at a redshift $z = 350$ when the fluctuations are still linear. The high resolution region forms the first non-linear structures at z=60 and the entire region quickly becomes distorted by the complex tidal field from the surrounding overdensities. By a redshift z=26 the high-resolution region begins to merge into the lower resolution surroundings and we do not analyse the region further, however this is sufficiently late that about 5 percent of the mass in the region has collapsed into bound dense structures (halos), see Figure 1.

The first dark matter halos to collapse and virialise are smooth triaxial objects of mass $10^{-6} M_{\odot}$ and half mass radii of 10^{-2} parsecs. Figure 2 shows the density profiles of three representative halos at z=26 which are well fitted by single power law density profiles $\rho(r) \propto r^{-\gamma}$ with slopes γ in the range from 1.5 to 2, similar to galactic halos shortly after their formation.[20] Note that the densities at the virial radius are about an order of magnitude higher than the density at $0.01 r_{\mathrm{virial}}$ in a galactic halo today, which makes the survival of many of these halos as galactic substructure possible. The central resolved densities reach 10^9 times the mean background density at one percent of their virial radii. Unlike galaxy and cluster mass CDM halos, they do not contain substructure since no smaller mass halos have collapsed in the hierarchy.

Figure 3 shows the mass function of halos. We use a friends of friends algorithm with a linking length set to identify the dense central regions of collapsed halos, then for each halo centre we recursively search for the radius r_{200} that is at an overdensity of 200 times the cosmic mean density. The resulting halo mass function is steep $dn(M)/d\log M \propto M^{-1}$. For comparison we plot an extrapolation of the halo mass function found on much larger scales $> 10^7 M_{\odot}$ [21] which fits surprisingly well up to the cut-off scale of $10^{-6} M_{\odot}$ below which we find no more structures.

At these epoch the baryons are kept sufficiently warm by the CMB that they are

unable to cool and form visible objects such as stars or planets within such tiny systems.[13] The dark halos may be detected via gravitational effects such as lensing or dynamical perturbations. Although we can not simulate the entire galactic halo at the resolution required to determine the survival statistics of these objects we can make some simple estimates of their survival and abundances. As the Galactic halo is assembled, these first objects merge successively into more massive systems. From scales of $10^7 M_\odot$ to $10^{15} M_\odot$ the mass function of substructure is a self similar power law of slope $dn(m)/dm \propto m^{-1.9}$ [22]. Extrapolating the subhalo mass function to the smallest scales gives us a total number of substructure halos $N(M > 10^{-6} M_\odot) \sim 5 \times 10^{15}$ and the expected number density of subhalos at the solar radius is $n(R_\odot) \approx 500 \text{pc}^{-3}$, assuming that they trace the mass. Although this extrapolation is made to much smaller masses than simulated previously, the substructure within halos collapsing at $z \approx 15$ with masses $\sim 10^7 M_\odot$ fit the extrapolation from larger mass scales[23] even though they form from regions of the CDM power spectra with effective index $n \approx -2.95$.

Can these structures survive the strong disruptive gravitational forces from the Galaxy? The tidal radius is simply the inner Lagrange point of the rotation of the two body system. For halos with power law density profiles $\rho(r) \propto r^{-2}$ we find $r_t = (R v_{sat})/(\sqrt{2} V_{parent})$ where v_{sat} and V_{parent} are the effective circular velocities $(V = \sqrt{GM/r})$ of the satellite and main halo and R is the pericentric distance of the satellite. For the smallest mini-halos $v_{sat} \approx 1\text{m/s}$, $r_{200} = 0.01$ parsecs. Therefore within the Galactic potential these halos could survive completely intact to about 3 kpc from the centre, well within the galacto-centric position of the sun. Encounters between halos and with stars and molecular clouds may disrupt a small fraction of these structures but using the impulsive heating approximation we estimate that most will survive with little mass loss.

A significant fraction of the mass may lie within bound structures at our location within the Galaxy, lowering the available smoothly distributed matter necessary for direct detection experiments. The earth passes through a dark matter mini-halo every 10,000 years, an encounter which lasts for about 50 years, therefore most of the time the earth is within an underdense region of dark matter. Integrating the mass function from $10^{-6} M_\odot$ to $10^{10} M_\odot$, normalised such that 10% of the mass is within substructure above a mass scale

of $10^7 M_\odot$ (as given by simulations of Galactic halos) we find that about 50 percent of the mass is bound to dark matter substructures. The velocity perturbation to a planetary orbit or satellite is very small ($\approx 10^{-6}$m/s), well below the observational constraints. However resonant encounters and the cumulative effects of $\approx 10^6$ impulsive encounters may cause significant perturbations to some of the bodies orbiting in the Oort cloud surrounding the solar system.

Compact objects in the mass range considered here could produce a microlensing signal in a multiply lensed quasar image, such as time varying flux differences.[24] The lensing object needs to be smaller than the Einstein radius

$$r_E = 3.7 \times 10^{16} \sqrt{\frac{M}{h M_\odot}} \text{ cm} \quad . \tag{1}$$

For a $10^{-6} M_\odot$ object $r_E \simeq 10^{-7}$ pc, which is much smaller than the size of the mini-halos considered here, therefore it is unlikely that gravitational lensing can provide a constraint on their presence, either in our halo or on cosmological path lengths to distant quasars.

Indirect detection is a more interesting possibility and several ongoing and planned experiments aim to detect the atmospheric Cerenkov light from gamma-rays produced by neutralino annihilation in the cores of dark halos halos.[7,25–28] Simple scaling arguments can show that minihalos can have high relative luminosities in γ-rays. The absolute γ-ray luminosity of a dark matter halo with an NFW density profile is proportional to $L \propto \rho_s^2 \, r_s^3$, where r_s is the scale radius of the NFW profile and $\rho_s = \rho(r_s)$.[29] The relative luminosity that would arrive at the detector from a halo at a distance d is then $L_{\rm rel} \propto L d^{-2}$.

Now we compare the relative luminosity of a minihalo at a distance of 0.1 parsec (their expected mean separation) to the signal from the centre of the Draco dwarf galaxy:

$$\frac{L_{\rm rel,mini}}{L_{\rm rel,draco}} \propto \left(\frac{7 \times 10^6 \rho_{\rm crit}}{1.7 \times 10^5 \rho_{\rm crit}} \right)^2 \left(\frac{0.005 \text{pc}}{300 \text{pc}} \right)^3 \left(\frac{0.1 \text{pc}}{82,000 \text{pc}} \right)^{-2} \approx 5 \tag{2}$$

where we used the typical minihalo properties from our simulations. The large abundance of the smallest subclumps compensates their smaller absolute luminosity and the closest of them will be bright sources of γ-rays. The background flux will be enhanced by a boost factor of over two orders of magnitude over a smooth Galactic dark matter potential. Current indirect detection experiments such as VERITAS,[26] HESS,[27] MAGIC[28] or CANGAROO-III[25] can probe part of the parameter space predicted by SUSY theory

by observing the galactic centre. However this region is dynamically complex since it contains numerous confusing astrophysical gamma ray sources and a supermassive black hole that can erase the central cusp. CDM mini-halos are potentially bright and will not suffer from these problems. All sky surveys could detect some nearby minihalos which would have a characteristic extent on the sky that is similar to that expected for a more distant satellite galaxy like Draco.

1. Peebles, P. J. E. Large-scale background temperature and mass fluctuations due to scale-invariant primeval perturbations *Astrophysical Journal* **263**, L1-L5 (1982).

2. Hofmann, S., Schwarz, D. J., & Stöcker, H. Damping scales of neutralino cold dark matter *Phys. Rev. D* **64**, 083507 (2001).

3. Berezinsky, V., Dokuchaev, V. & Eroshenko, Y. Small-scale clumps in the galactic halo and dark matter annihilation. *Phys. Rev. D* **68**, 103003 (2003).

4. Green, A. M., Hofmann, S. & Schwarz, D. J. The power spectrum of SUSY-CDM on sub-galactic scales. *Mon. Not. Roy. Astron. Soc.* **353**, L23-L27 (2004).

5. Jungman, G., Kamionkowski, M., & Griest, K. Supersymmetric dark matter *Physics Reports* **267**, 195-373 (1996).

6. Ellis J. R., Olive K. A. & Santoso Y. Constraining supersymmetry. *New J. Phys.* **4**, 32 (2002).

7. Bertone, G., Hooper, D. & Silk, J. Particle dark matter: Evidence, candidates and constraints. Preprint at ¡http://arXiv.org/astro-ph/0404175¿ (2004).

8. Spergel, D. N., et al. First-Year Wilkinson Microwave Anisotropy Probe (WMAP) Observations: Determination of Cosmological Parameters. *Astrophys. J. Supp.* **148**, 175-194 (2003).

9. Riess A. G., et al. Observational Evidence from Supernovae for an Accelerating Universe and a Cosmological Constant *Astron. J.* **116**, 1009-1038 (1998).

10. Perlmutter S., et al. Measurements of Omega and Lambda from 42 High-Redshift Supernovae *Astrophys. J.* **517**, 565-586 (1999)

11. Tegmark, M., et al. Cosmological parameters from SDSS and WMAP. *Phys. Rev. D* **69**, 103501 (2004).

12. Peebles, P. J. E. Dark matter and the origin of galaxies and globular star clusters *Astrophysical Journal* **277**, 470-477 (1984).

13. Tegmark, M., Silk, J., Rees, M. J., Blanchard, A., Abel, T., & Palla, F. How Small Were the First Cosmological Objects? *Astrophysical Journal* **474**, 1-12 (1997).

14. Turner, M. The Case for Omega mass = 0.33 +/- 0.035 *Astrophysical Journal* **576**, L101-L104 (2002).

15. Lake, G. Detectability of gamma-rays from clumps of dark matter. *Nature* **346**, 39L-40L (1990).

16. Bergstrom, L., Edsjo, J., Gondolo, P. & Ullio, P. Clumpy neutralino dark matter. *Phys. Rev. D* **59**, 043506 (1999).

17. Calcáneo-Roldán C., Moore B. Surface brightness of dark matter: Unique signatures of neutralino annihilation in the galactic halo. *Phys. Rev. D* **62**, 123005, (2000).

18. Prada, F., Klypin, A., Flix, J., Martinez, M. & Simonneau, E. Astrophysical inputs on the SUSY dark matter annihilation detectability. Preprint at ¡http://arXiv.org/astro-ph/0401512¿ (2004).

19. Bertschinger, E. Multiscale Gaussian Random Fields and Their Application to Cosmological Simulations *Astrophys. J. Supp.* **137**, 1-20 (2001).

20. Tasitsiomi, A., Kravtsov, A. V., Gottlober, S. & Klypin, A. A. Density profiles of LCDM clusters. *Astrophys. J.* **607**, 125-139 (2004).

21. Reed, D. *et al.* Evolution of the mass function of dark matter haloes. *Mon. Not. Roy. Astron. Soc.* **346**, 565-572 (2003).

22. Diemand, J., Moore, B. & Stadel, J. Velocity and spatial biases in cold dark matter subhalo distributions. *Mon. Not. Roy. Astron. Soc.* **352**, 535-546 (2004).

23. Moore, B. *et al.* Dark matter in Draco and the Local Group: Implications for direct detection experiments *Phys. Rev. D* **64**, 063508 (2001).

24. Schmidt, R. & Wambsganss, J. Limits on MACHOs from microlensing in the double quasar Q0957+561 *Astronomy & Astrophysics* **335**, 379-387 (1998).

25. Mori, M. *et al.* [The CANGAROO Collaboration], Status of the CANGAROO-III project. *AIP Conf. Proc.* **558**, 578-581 (2001).

26. Cogan, P. *et al.* [The VERITAS Collaboration]. An overview of the VERITAS prototype telescope and camera. Preprint at ¡http://arXiv.org/astro-ph/0408155¿ (2004).

27. Hinton, J .A. *et al.* [The HESS Collaboration]. The status of the HESS project. *New Astron. Rev.* **48**, 331-337 (2004).

28. Cortina, J. *et al.* [The MAGIC Collaboration]. Status and First Results of the MAGIC Telescope. Preprint at ¡http://arXiv.org/astro-ph/0407475¿ (2004).

29. Koushiappas, S. M., Zentner, A. R. & Walker, T. P. Observability of gamma rays from neutralino annihilations in the Milky Way substructure *Phys. Rev. D* **69**, 043501 (2004).

30. Diemand, J., Moore, B. & Stadel, J. Convergence and scatter of cluster density profiles. *Mon. Not. Roy. Astron. Soc.* **353**, 624-632 (2004).

Please address all correspondence and requests for materials to Professor Ben Moore.
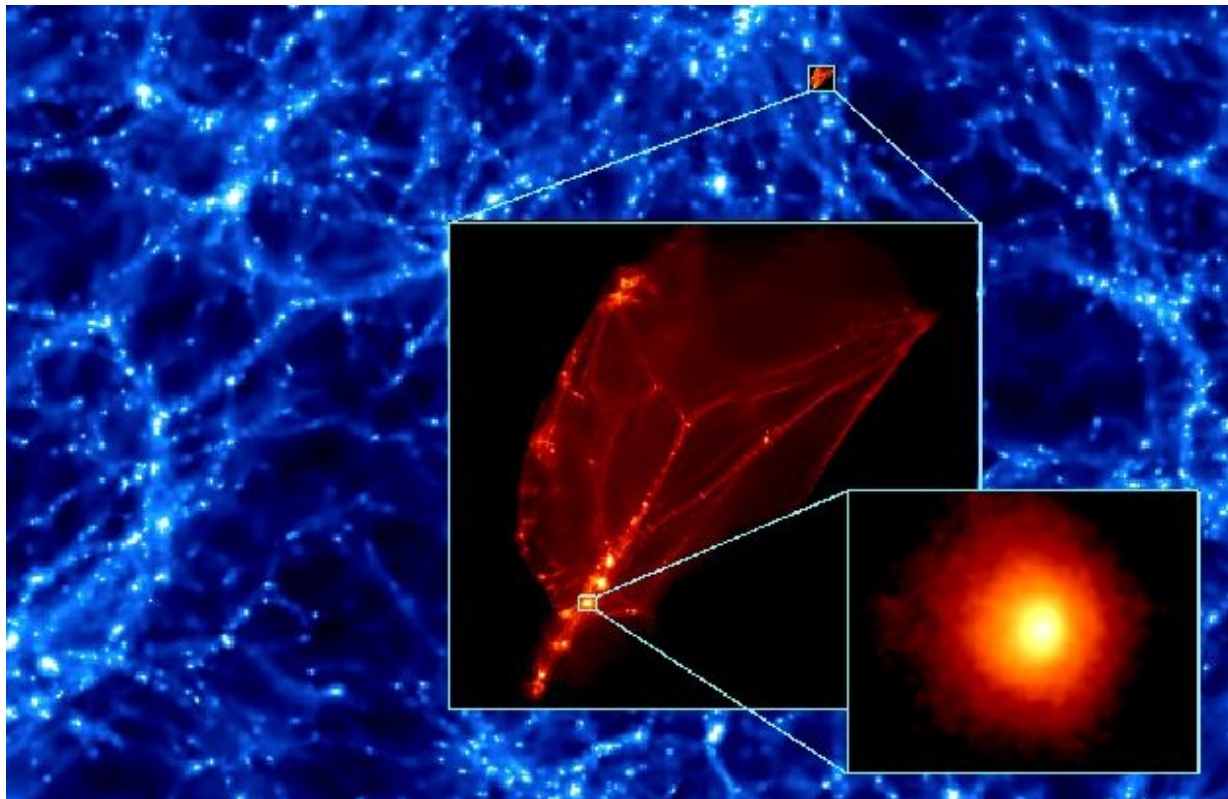
Acknowledgements

Figure 1. A zoom into one of the first objects to form in the universe. The colours show the density of dark matter at redshift 26. Brighter colours correspond to regions of higher concentrations of matter. The blue background image shows the small scale structure in the top cube (cube size $=$ [3 comoving kpc]^3) which has a similar filamentary topology as the large scale structure in the CDM universe. The first red image zooms by a factor of one hundred into the average density high resolution region. This region was initially a cube of [60 comoving pc]^3 resolved with 64 million particles with a gravitational softening of 10^{-2} comoving parsecs and masses $1.2 \times 10^{-10} M_\odot \equiv M_{moon}/300$. The final image shows a close up of one of the individual dark matter halos in this region, again zooming in by a factor of one hundred so that the box has a physical length of 0.024 parsecs. This tiny triaxial Earth mass halo has a cuspy density profile and is smooth, devoid of the substructure that is found within galactic and cluster mass dark matter halos. Even though the index of the power spectrum is very steep on these scales, $n \approx -3$, we find that halos can collapse before merging into a larger system, rather than the niave expectation that all scales are collapsing simultaneously thus erasing such structures.
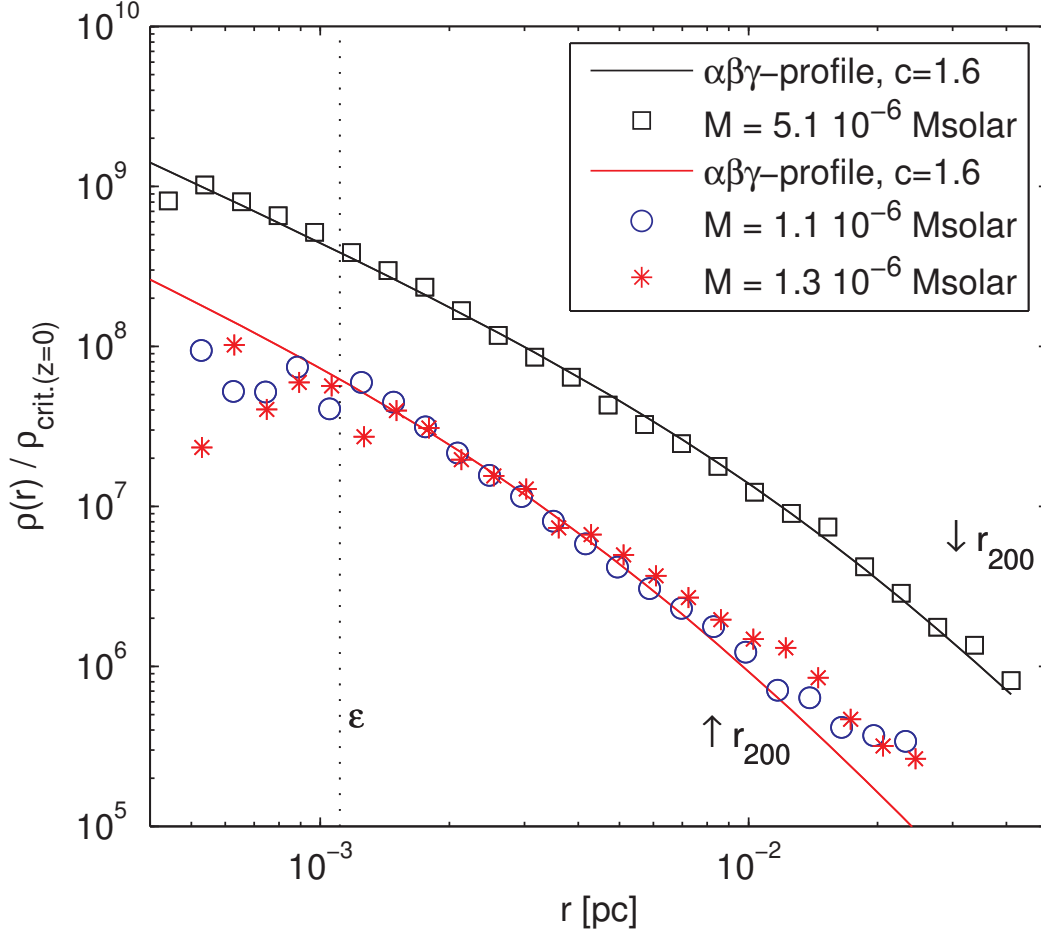
Figure 2. Radial density profiles of three typical minihalos at redshift 26. The radial distance is plotted in physical units and we show low concentration $\alpha\beta\gamma$-profiles for comparison. We use the mean dark matter profile infered from the highest resolution galaxy cluster simulations,[30] i.e. $(\alpha\beta\gamma) = (1, 3, 1.2)$. The vertical dotted line indicates our force resolution and the arrows indicate the radii that is 200 times the background density. Across the entire range of halo masses from 10^{-6} to $10^1 M_\odot$, we find small concentration parameters $c < 3$. We do not observe a trend of concentration with mass, possibly because the halos all form at a similar epoch as expected when the power spectrum is so steep.
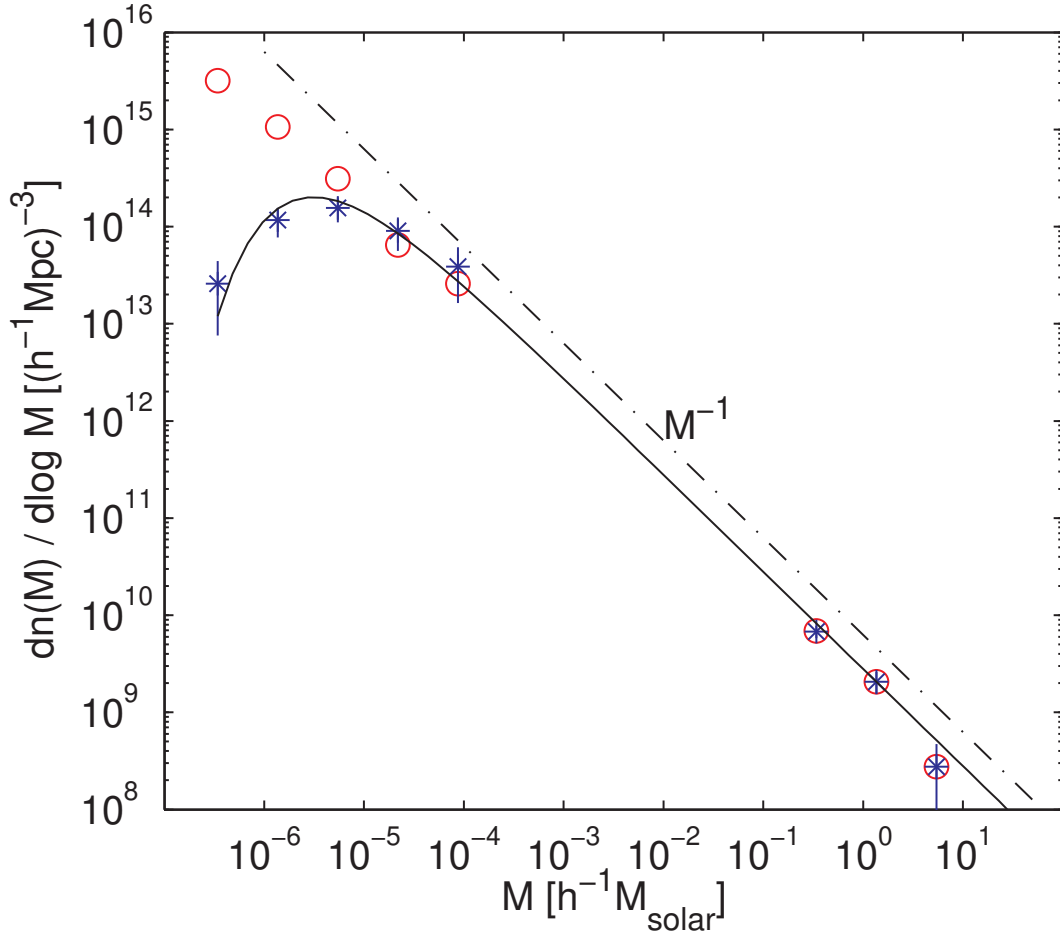
Figure 3. The abundance of collapsed and virialised dark matter halos of a given mass. The same region was simulated twice using different types of intial fluctuations: (A) SUSY-CDM with a 100 GeV neutralino (stars) and (B) an additional model with no small scale cut-off to the power spectrum (open circles) as might be produced by an axion dark matter candidate. Densities are given in co-moving units, masses in $h^{-1}\mathrm{M}_\odot = 1.41\mathrm{M}_\odot$, where $h = 0.71$ is the normalized present day Hubble expansion rate. Model (B) has a steep mass function down to the resolution limit whereas run (A) has many fewer halos below a mass of about $5 \times 10^{-6}h^{-1}\mathrm{M}_\odot = 3.5 \times 10^{-6}h^{-1}\mathrm{M}_\odot$. (Our simulations do not probe the mass range from about $3 \times 10^{-4}h^{-1}\mathrm{M}_\odot$ to $2 \times 10^{-1}h^{-1}\mathrm{M}_\odot$.) The dashed-dotted line shows an extrapolation of the number density of galaxy halos (from[21]) assuming $dn(M)/d\log M \propto M^{-1}$. The solid line is the function $dn(M)/d\log M = 2.8 \times 10^9 (M/h^{-1}\mathrm{M}_\odot)^{-1} \exp[-(M/M_\mathrm{cutoff})^{-2/3}](h^{-1}Mpc)^{-3}$, with a cutoff mass $M_\mathrm{cutoff} = 5.7 \times 10^{-6}h^{-1}\mathrm{M}_\odot$. The power spectrum cutoff is $P(k) \propto \exp[-(k/k_{fs})^2]$, where k_{fs} is the free streaming scale and assuming $k \propto M^{-1/3}$ motivates the exponent of $-2/3$ in our fitting function.